Journal of Quantitative Spectroscopy & Radiative Transfer 226 (2019) 81–86

Contents lists available at ScienceDirect

Journal of Quantitative Spectroscopy & Radiative Transfer

journal homepage: www.elsevier.com/locate/jqsrt

Spherical particle absorption over a broad range of imaginary refractive index

Christopher M. Sorensen[a,*], Justin B. Maughan[a], Hans Moosmüller[b]

[a] Department of Physics, Kansas State University, 116 Cardwell Hall, 1228 N. 17th Street, Manhattan, KS 66506, USA
[b] Laboratory for Aerosol Science, Spectroscopy, and Optics, Desert Research Institute, Nevada System of Higher Education, 2215 Raggio Parkway, Reno, NV 89512, USA

ARTICLE INFO

Article history:
Received 19 November 2018
Revised 9 January 2019
Accepted 10 January 2019
Available online 11 January 2019

Keywords:
Absorption
Complex refractive index
Mie theory
Rayleigh theory

ABSTRACT

This paper presents studies of the optical absorption cross section for homogeneous spheres of radius R interacting with light of wavelength λ as calculated with the Mie equations. Four regimes of behavior are disclosed: the Rayleigh Regime, the Geometric Regime, the Reflection Regime, and a Crossover Regime. Two parameters govern these regimes, the imaginary part of the refractive index, κ, and the product of κ with the sphere size parameter kR where $k=2\pi/\lambda$, i.e. κkR. Simple, approximate functionalities on κ, k, sphere volume and projected geometric cross section are derived for these regimes. Interesting aspects of our observations include: Rayleigh absorption can apply to all particle sizes, Fresnel reflection can occur for sub-wavelength spheres, and while κ is the agent of absorption, large κ can increase scattering to the detriment of absorption.

1. Introduction

All material objects have a wavelength dependent complex refractive index $m=n+i\kappa$. In general, the real part n dominates the refraction and speed of light, and the imaginary part κ dominates the absorption of light; both factor approximately equivalently into the reflection of light. Studies of optical properties typically pay more attention to the real part n than to the imaginary part κ. This is understandable, because one is often dealing with transmissive optics, and when dealing with reflective optics, reflection coefficients are used as the relevant parameters, not κ nor n. Moreover, in many situations κ is small. But such a statement, as we shall see, can be problematic in itself because it engenders the question "small compared to what?".

In this paper we explicitly consider the effects of the imaginary refractive index κ on the absorption properties of spheres. We will consider very wide ranges of κ and sphere size parameters kR, where $k=2\pi/\lambda$, λ being the wavelength of light and R the sphere radius.

Our method is simple: we use the Mie equations (e.g., [1]) to calculate the absorption cross section. Our approach is surprisingly novel: we plot the absorption cross section versus the imaginary part of the refractive index, κ. Because κ is the cause of the absorption, this is a very reasonable approach.

2. Results

Fig. 1 shows the absorption cross section C_{abs} for a sphere of radius R as a function of the imaginary refractive index κ for a wide range of size parameters kR where $k=2\pi/\lambda$ and λ is the wavelength of light. The real part of the refractive index is constant at $n=1.5$. The figure shows that when the imaginary refractive index κ is small, the absorption cross section increases linearly with κ for all sizes. For large sizes such that $kR>1$ this increase levels of when $\kappa \gtrsim 1/kR$, i.e., when the parameter $\kappa kR \gtrsim 1$, $C_{abs} \simeq G=\pi R^2$, the geometric cross section. Continuing with $kR>1$, when $\kappa>2$, the absorption falls off with the square of κ. In contrast, for smaller particles, when $kR<1$, the absorption cross section never reaches the geometric cross section from its linear ascent from small κ. Instead near $\kappa \simeq 1$, it begins to decrease, eventually gaining an inverse cubic dependence on κ. This decrease is interrupted near $\kappa kR \simeq 0.3$ where an inflection occurs, after which, near $\kappa kR \simeq 3$ at large κ, the same quadratic decrease with κ as seen for large sizes develops. We have replotted Fig. 1 for $n=1.1$ and 3 and found very similar trends.

To bring some order to this remarkable (to us) series of functionalities, we will divide Fig. 1 into four regimes:

1. The Rayleigh Regime when $\kappa kR<0.3$.
2. The Geometric Regime when $kR>1$ and $\kappa kR>1$ and $\kappa<1$.
3. The Reflection Regime when $\kappa>3$ and $\kappa kR>3$.
4. The Crossover Regime when $0.3<\kappa kR<3$ and $kR<1$.

* Corresponding author.
E-mail address: sor@phys.ksu.edu (C.M. Sorensen).

https://doi.org/10.1016/j.jqsrt.2019.01.011
0022-4073/

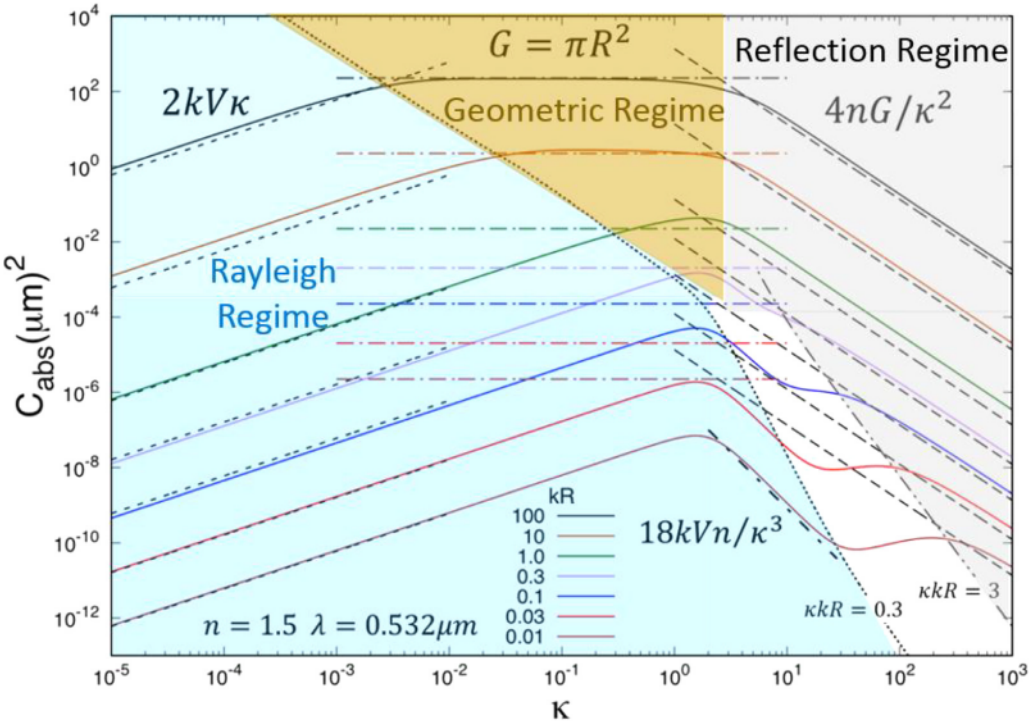

Fig. 1. Spherical particle absorption cross section C_{abs} as a function of the imaginary refractive index κ. Seven different particle size parameters kR are shown. The light wavelength is $\lambda = 0.532\,\mu m$ and the real part of the refractive index is constant at $n = 1.5$. Dashed lines show the functionalities $2kV\kappa$ and $4nG/\kappa^2$ as marked; horizontal dot-dash lines indicate $C_{abs} = G = \pi R^2$, and short dot-dash line shows the functionality $18kVn/\kappa^3$ as marked. Dotted line and dash-double-dot line mark the boundaries of the crossover regime at $\kappa kR = 0.3$ and 3.0, respectively. Shaded areas indicate the Rayleigh, Geometric, and Reflection Regimes. The unshaded area is the Crossover Regime.

We intend to study each of these regimes below, but first we will describe the importance of the parameter κkR.

2.1. The parameter κkR

The parameter κkR was first described in [2]. It was discovered that the combination κkR universally parameterized changes in the angular scattering behavior of spheres, whereas the individual κ and kR do not. The parameter has been shown to apply to non-spherical ice crystals [3], and its usefulness has been described in a recent review [4].

The universality of this parameter has a simple physical basis. When the refractive index of a medium has a non-zero imaginary part, i.e., when $\kappa > 0$, light will decay exponentially as it propagates into a uniform and homogeneous medium with a 1/e ≃ 0.37 decay length of

$$\delta = 1/(\kappa k_{vac}) = \lambda_{vac}/(2\pi\kappa), \tag{1}$$

where the subscript "vac" means "vacuum". The parameter δ is often called the *skin depth* [5]. The ratio of the sphere radius to the skin depth, R/δ is κkR, i.e.,

$$R/\delta = \kappa kR. \tag{2}$$

Thus κkR quantifies the relative extent of the light penetration into the sphere. When $\kappa kR << 1$, absorption does not impede the entering wave from affecting the entire volume of the sphere. When $\kappa kR > 1$, absorption causes the light to be confined to near the surface of the sphere. From a perspective relevant here, κkR determines whether the absorption is affected by the volume of the sphere or by the near-surface region of the sphere. The parameter also answers, to some degree, the question for the dimensionless κ, "small compared to what?" It's not the magnitude of κ that matters, but rather the magnitude of the dimensionless κkR compared to one.

2.2. The Rayleigh regime $\kappa kR < 0.3$

Here we will show that all the spheres, regardless of size, display a semi-quantitative Rayleigh theory dependence of absorption cross section on κ when the parameter $\kappa kR < 0.3$. The canonical definition of the Rayleigh regime is constrained with two conditions [6], $kR << 1$ and $kR|m| << 1$. Note that the first condition restricts particle size to be much smaller than the wavelength, thereby ensuring constructive interference with very little phase shift for the scattered light, yielding the V^2 dependence of the scattering cross-section [7,8]. However, absorption is an incoherent process, not dependent on phase shifts. Therefore, the first condition does not directly affect the absorption cross section. The latter condition addresses absorption in the Rayleigh regime, ensuring that the incident light fully penetrates the particle volume and yielding the V dependence of the absorption cross-section, consistent with our $\kappa kR < 0.3$ [9]. The Rayleigh absorption cross section is given by [6]

$$C_{abs\ Rayleigh} = 4\pi R^2 (kR) E(m) = 3VkE(m), \tag{3}$$

where

$$E(m) = Im\left[\frac{m^2 - 1}{m^2 + 2}\right]. \tag{4}$$

Note the volume dependence V in Eq. (3). If $\kappa < 1$, the Rayleigh absorption cross section becomes

$$C_{abs\ Rayleigh\ small\ \kappa} \simeq 18kVn\kappa/\left(n^2 + 2\right)^2. \tag{5}$$

Eq. (5) has the linear dependence with κ seen in Fig. 1 that was obtained from Mie theory. Eq. (5) can be simplified further by setting the real refractive index $n = 1.0$ to obtain

$$C_{abs\ Rayleigh\ small\ \kappa}(n = 1.0) \simeq 2kV\kappa. \tag{6}$$

This result is included in Fig. 1 as a dashed line and seen to be in semi-quantitative agreement with the Mie result for all size

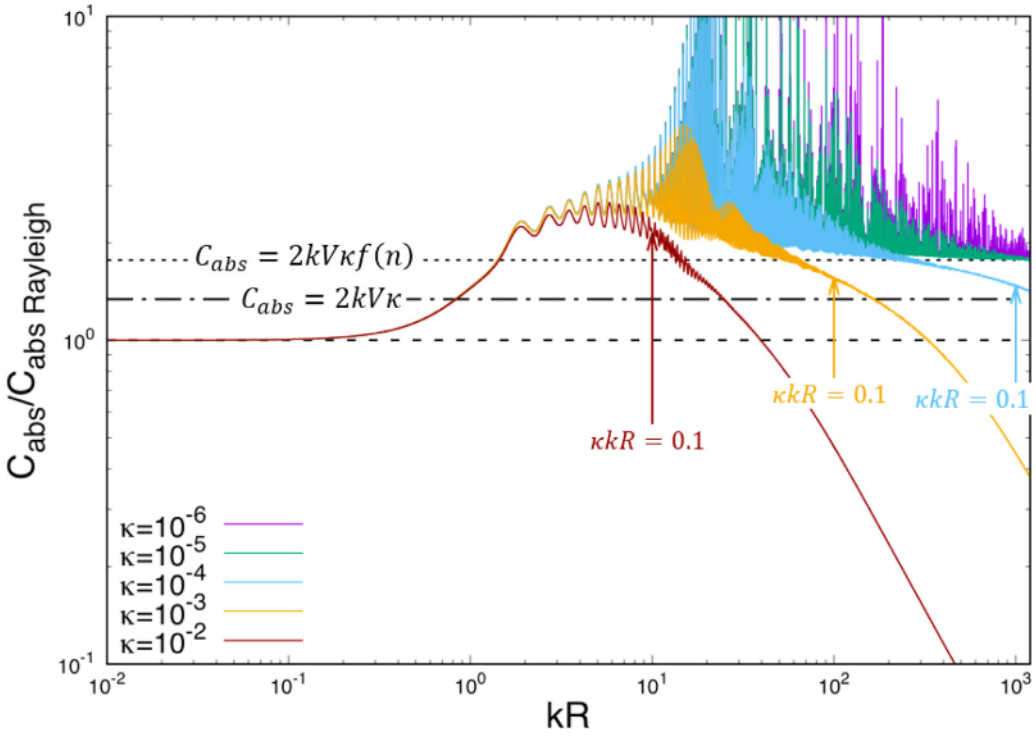

Fig. 2. The ratio of the absorption cross section calculated with the Mie equations for spheres divided by the exact Rayleigh theory predictions of Eqs. (3) and (4) versus the size parameter kR. The light wavelength is $\lambda = 0.532\,\mu m$ and the real part of the refractive index is $n = 1.5$. Plots are made for a wide range of imaginary refractive indices, $\kappa < 1$. The dashed line indicates where this ratio is 1.0, the dot-dashed line indicates the ratio of $C_{abs} = 2kV\kappa$ (also used in Fig. 1), Eq. (6), to the Rayleigh theory prediction, and the short-dashed line indicates the ratio of $C_{abs} = 2kV\kappa f(n)$, Eq. (8), to the Rayleigh theory prediction. Note that some of the spike-like structure may be affected by aliasing.

parameters as long as $\kappa kR < 0.3$ and $\kappa < 1$. Note that when $n = 1.5$, Eq. (5) leads to $C_{abs\ Rayleigh\ small\ \kappa}(n = 1.5) \simeq 1.49kV\kappa$.

On the other hand when $\kappa > 1$, the Rayleigh absorption cross section becomes

$$C_{abs\ Rayleigh\ large\ \kappa} \simeq 18kVn/\kappa^3. \tag{7}$$

This result is also included in Fig. 1 as a short dot-dash line and seen to be in semi-quantitative agreement with the Mie result for all small size parameters, $\kappa > 3$ and $\kappa kR < 0.3$. Note that although $\kappa >> 1$, $\kappa kR < 1$ so the entire volume of the sphere is still nearly-uniformly illuminated to yield a volume dependence in Eq. (7). To recap, we find that the Rayleigh theory-derived Eqs. (6) and (7) apply semi-quantitatively for particles of all sizes when $\kappa kR < 0.3$ and κ is either much less than or much greater than approximately one, respectively.

Fig. 2 compares the Mie result to the Rayleigh theory predictions by plotting the Mie calculated absorption cross section divided by the Rayleigh theory prediction of Eqs. (3) and (4). There we see that when $kR \lesssim 1$, the Rayleigh and Mie theory predictions agree as expected. In the other extreme when $kR \gtrsim 100$, Rayleigh theory under-predicts the absorption cross section by about a factor of two as long as $\kappa kR \lesssim 0.01$. Nevertheless, the two are proportional. When $1 \lesssim kR \lesssim 100$ and $\kappa kR \lesssim 0.01$, Rayleigh theory not only under-predicts but it misses a strong ripple structure in the Mie result. For all kR the ratio of Mie and Rayleigh theory calculated absorption declines rapidly after $\kappa kR \gtrsim 0.1$. When $\kappa kR \gtrsim 1$, the ratio falls off linearly with kR, consistent with the transition of the absorption cross section from a volumetric to the geometric cross sectional area dependence seen in Fig. 1.

Bohren and Huffman [6] used a geometric optics approach to derive a formula for the absorption cross section valid for large size parameters and weakly absorbing spheres. Their result is

$$C_{abs\ B\&H} = 2kV\kappa\left\{n^{-1}\left[n^3 - \left(n^2-1\right)^{3/2}\right]\right\} = 2kV\kappa f(n). \tag{8}$$

Note that the same product $kV\kappa$ included in this equation also appears in Eqs. (5) and (6). When $n = 1.0$, the bracketed term in Eq. (8) (i.e., f(n)) equals 1, so that Eq. (8) becomes identical to Eq. (6), which was derived from the Rayleigh theory cross section in the $n \to 1$ limit. For $n = 1.5$ the bracketed term f(n) = 1.318 and inclusion of this factor yields perfect agreement between Eq. (8) and the ratio $C_{abs}/C_{abs\ Rayleigh}$ plotted in Fig. 2 for large kR and $\kappa kR < 0.01$.

All these results show that in the regime where $\kappa kR < 0.3$ the Rayleigh theory equations for absorption yield the correct functionality of $kV\kappa$ and give magnitudes in semi-quantitative agreement with Mie theory and geometric optics calculations. Keep in mind that this statement applies to both small and large size parameters so long as $\kappa kR < 0.3$, i.e., $\kappa < 1/3kR$. Under this condition, the absorbance does not significantly affect the light propagation into the volume of the sphere.

2.3. The geometric regime when $kR > 1$ and $\kappa kR > 1$ and $\kappa < 1$

Fig. 1 shows a geometric regime occurs such that the absorption cross section C_{abs} is approximately equal to the geometric cross section, $G = \pi R^2$, when $kR > 1$ and $\kappa kR > 1$ and $\kappa < 1$.

Fig. 3 explores the accuracy of $C_{abs} = G$ in more detail and from a different perspective by plotting the absorption efficiency $Q_{abs} = C_{abs}/G$ versus the size parameter kR. There we see that for large kR, $C_{abs} = G$ is fulfilled fairly well when $\kappa kR > 1$, while κ varies over orders of magnitude. However, this agreement diminishes as κ increases through unity. When $\kappa = 10$, the Mie calculated absorption cross section is more than an order of magnitude smaller than the geometric cross section (i.e., $Q_{abs} < 0.1$). Arrows

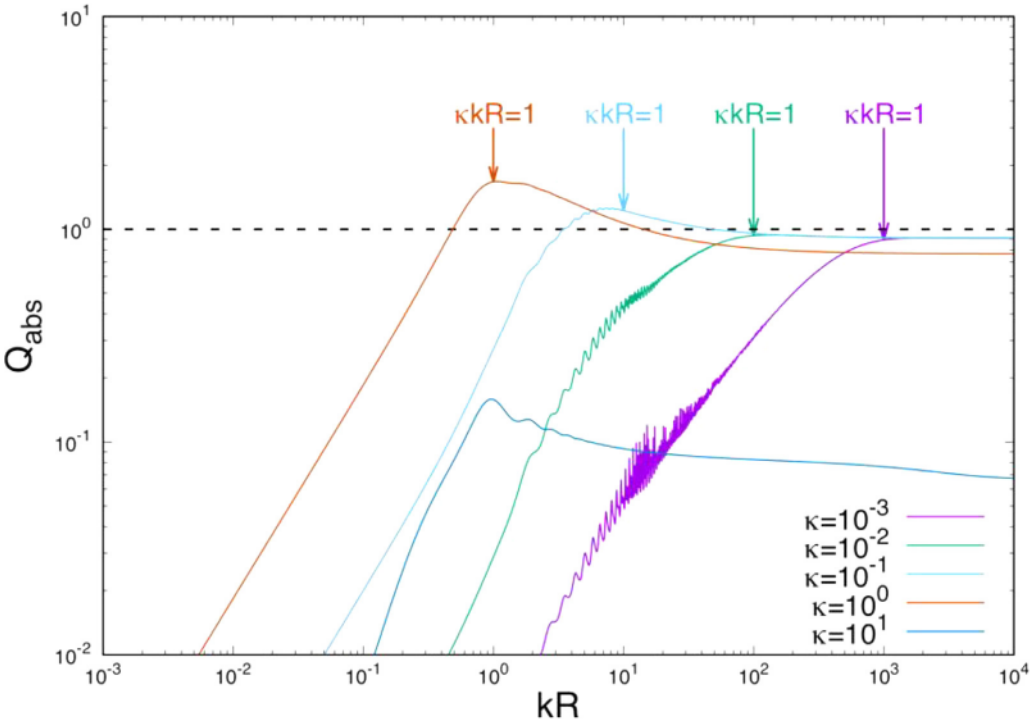

Fig. 3. The absorption efficiency $Q_{abs} = C_{abs}/G$ calculated with the Mie equations for spheres versus the size parameter kR. The light wavelength is $\lambda = 0.532\,\mu m$ and the real part of the refractive index is $n = 1.5$. Plots are made for a wide range of imaginary refractive indices, κ. Arrows indicate where $\kappa kR = 1$ for different κ.

indicating where $\kappa kR = 1$ emphasize the importance of the parameter κkR by indicating the crossover from volumetric dependent Rayleigh regime to the surface dependent geometric regime that results in the geometric cross section.

2.4. The reflection regime when $\kappa > 3$ and $\kappa kR > 3$

Fig. 1 shows that a third regime occurs whenever $\kappa > 3$ and $\kappa kR > 3$. In this regime the absorption cross section falls from the geometric limit quadratically with increasing κ. Also, it is well known that for large size parameters the extinction cross section, which is the sum of the absorption and scattering cross sections, i.e., $C_{ext} = C_{abs} + C_{sca}$, approaches 2 G as $kR \to \infty$. Thus when $kR > 1$, so that $C_{abs} + C_{sca} \simeq 2G$, if C_{abs} decreases from G with increasing κ, C_{sca} must increase from G with increasing κ. The conclusion is that as κ passes from 1 to 10 or more, absorption gives way to specular reflection to keep the extinction cross section equal to 2 G. One can envision that a smooth, black sphere with $C_{abs} = \pi R^2$ becomes shiny like a steel ball as κ increases beyond ~ 3. Note that reflection is a form of scattering so, ironically, the parameter that causes absorption, κ, ultimately causes scattering and quenches absorption!

With these thoughts in mind, consider large spheres and apply geometric optics to determine their scattering cross section C_{sca}. For large spheres in the geometric optics regime, the scattering cross section can be written as the sum of scattering cross sections for diffraction, transmission, and surface reflection (ignoring internal reflections) as [10]

$$C_{sca} = C_{sca\_D} + C_{sca\_T} + C_{sca\_R}, \tag{9}$$

where C_{sca_D} approaches G as $kR \to \infty$, C_{sca_T} becomes 0 for large κkR, and C_{sca_R}, the scattering cross section due to reflection from the sphere can be calculated using geometric optics by integrating the Fresnel reflection coefficients over a spherical surface as [10,11]

$$C_{Sca\_R} = \frac{G}{4}\int_0^{\pi} d\theta \sin(\theta) \left\{ \left(\frac{[\sin(\theta/2) - u_R]^2 + v_R^2}{[\sin(\theta/2) + u_R]^2 + v_R^2} \right) + \frac{[(n^2 - \kappa^2)\sin(\theta/2) - u_R]^2 + [2n\kappa \sin(\theta/2) - v_R]^2}{[(n^2 - \kappa^2)\sin(\theta/2) + u_R]^2 + [2n\kappa \sin(\theta/2) + v_R]^2} \right\} \tag{10}$$

where the two fractions in the large, round brackets contain the s- and p-polarized contributions, respectively, and u_R, v_R, and a are defined as

$$u_R = \sqrt{\frac{\sqrt{a^2 + (2n\kappa)^2} + a}{2}} \tag{11}$$

$$v_R = \sqrt{\frac{\sqrt{a^2 + (2n\kappa)^2} - a}{2}} \tag{12}$$

$$a = n^2 - \kappa^2 - \cos^2(\theta/2). \tag{13}$$

Here, the total reflectance $\boldsymbol{R}$ equals the scattering efficiency due to reflection $Q_{sca\_R}, = C_{sca\_R}/G$. The large, absorbing sphere is reflecting light from its surface, thus the "reflectance" absorption cross section is

$$C_{abs\ refl} = G(1 - \boldsymbol{R}) \tag{14}$$

This equation essentially claims that if the light reflects, it doesn't get absorbed.

The prediction of Eqs. (10) through (14) is compared to the exact Mie prediction as a ratio in Fig. 4. The prediction is shown to work well for $kR > 10$ and $\kappa > 3$ and becomes equal to the Mie prediction as both of these quantities grow larger. There is a hump in the ratio near $kR \simeq 1$. The prediction continues to work well when $kR < 1$, as long as $\kappa kR \gtrsim 10$. This is remarkable because the concept of geometric, specular reflection at the foundation of our prediction is surprising for subwavelength-size particles with $kR < 1$.

Eqs. (10) through (14) are complex, so we now attempt a simpler description. We will assume that the incident side of the sphere is flat with area $G = \pi R^2$ perpendicular to the incident light.

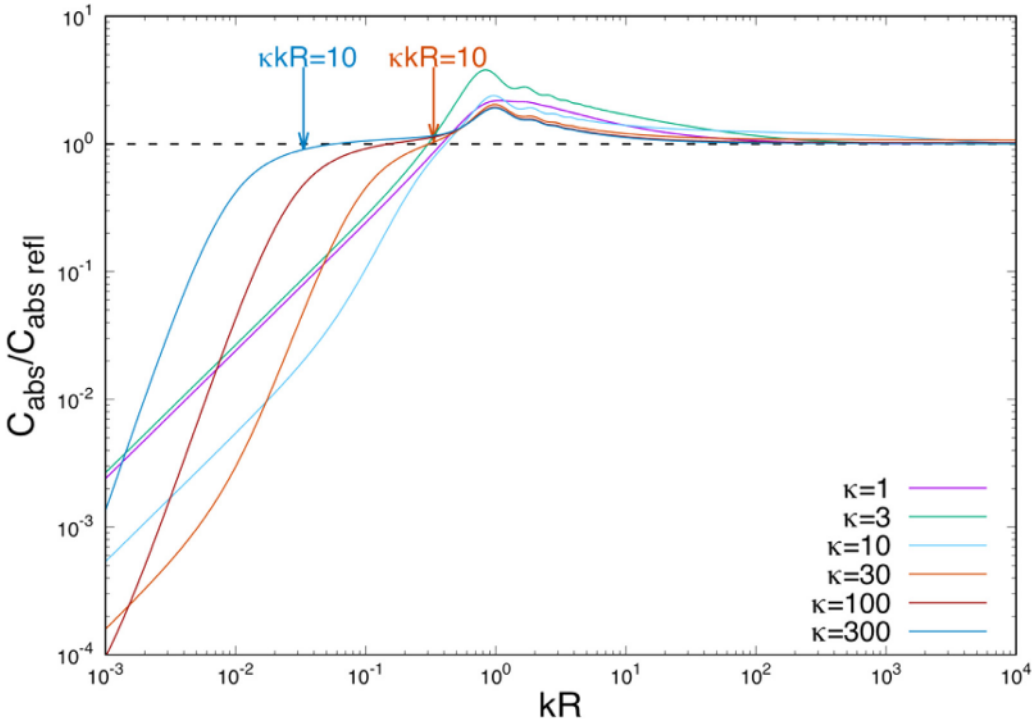

Fig. 4. The ratio of the absorption cross section calculated with the Mie equations for spheres divided by the reflectance absorption cross section of Eqs. (10) through (14) versus the size parameter kR. The light wavelength is 0.532 μm and the real part of the refractive index is $n = 1.5$. The dashed line indicates where the ratio is one. Plots are made for a wide range of imaginary refractive indices, κ.

Then we apply Fresnel reflection at normal incidence, where the reflectivity is

$$R = \frac{(n-1)^2 + \kappa^2}{(n+1)^2 + \kappa^2}. \tag{15}$$

With this, Eq. (14) becomes the "normal reflectance" absorption cross section

$$C_{abs\ norm\ refl} \simeq G\frac{4n}{(n+1)^2 + \kappa^2}. \tag{16}$$

In the limit of large κ such that $\kappa >> n$,

$$C_{abs\ norm\ refl} \simeq 4nG/\kappa^2. \tag{17}$$

The functionality of Eq. (17) is plotted in Fig. 1 and seen to provide an adequate description of the Mie calculated results for C_{abs} when $\kappa \gtrsim 3$. In particular, the normal reflectance absorption cross section of Eq. (17) successfully predicts the dependence on G and the inverse square dependence on κ and demonstrates them explicitly. This latter fact is not explicitly demonstrated by the more accurate reflectance absorption cross section of Eqs. (10) through (14). A more detailed comparison of Eq. (17), not shown here, shows that in the limit of $\kappa \to \infty$, Eq. (17) under-predicts the reflectance absorption cross-section result from Eqs. (10) through (14) by about 33% for all kR, and hence misses the Mie prediction by the same amount.

2.5. The crossover regime when $0.3 < \kappa kR < 3$ and $kR < 1$

In light of the results above, this regime occurs because small particles in the Rayleigh regime, $kR|m| \simeq \kappa kR < 1$, in which the entire volume of the particle is nearly uniformly illuminated by the incident light, hence obey Eq. (7), cross over to surface influenced interactions when $\kappa kR > 1$. Because the other condition for Rayleigh scattering still holds, viz. $kR < 1$, κ is quite large, e.g., $\kappa > 3$. This large κ leads to Fresnel reflection from these subwavelength particles and the functionality of Eq. (17).

2.6. Other features

Fig. 2 displays both a broad hump and rapid, high-frequency ripple features when the size parameter is in the range $1 \lesssim kR \lesssim 30$. These features are usually referred to as the interference and ripple structures, respectively, and are readily seen in plots of the scattering and extinction efficiencies [6,12]. The ripple structure can make C_{abs} very large. Figs. 3 and 4 also display a hump near $kR \simeq 1$.

Careful inspection of Figs. 2 and 3 shows that the ripple structure begins to disappear when $\kappa kR \simeq 0.01$ and is essentially gone when $\kappa kR \simeq 0.1$, regardless of the particular values of κ or kR. This is consistent with the physical picture of the source of the ripple structure being resonances of internal rays propagating along the inner circumference of the sphere and with the physical picture that κkR is a measure of the relative size path length in the sphere to the 1/e propagation length δ due to absorption. In fact, the relevant ratio for the internal modes would be the sphere circumference $2\pi R$ divided by δ to yield $2\pi\kappa kR$. Therefore, we can restate that the ripple structure begins to disappear when $2\pi\kappa kR \simeq 0.06$ and is essentially gone when $2\pi\kappa kR \simeq 0.6$.

The broad hump interference structure begins near $kR \simeq 1$ and dies away as κkR increases through ~ 0.1. The interference structure has been explained as being due to interference between light that has been diffracted by the particle with that which has passed through the particle [13–16]. The "ebbing away" of the broad hump with increasing κkR is consistent with a picture of light no longer passing through the particle at large κkR.

3. Discussion

When light encounters an object, it can either scatter via reflection, refraction, and diffraction of its energy, or the energy can be absorbed and converted to another form. In this work we have studied absorption and found various regimes of behavior. In some

cases these regimes imply surprising explanations and reflect on the behavior of scattering as well. We discuss these situations here.

Our results show that the Rayleigh regimes for absorption and scattering are different. Rayleigh scattering can be derived under the assumption that the particle's internal field is homogeneous. Then the particle acts like an oscillating dipole for which the re-emission of radiation, the scattering, can be calculated [1]. One condition for a homogeneous internal field is for the particle to be small compared to the wavelength, i.e. $kR \ll 1$. The role of refractive index can be shown via an electrostatics approach used by Bohren and Huffman [6] who considered the real and imaginary parts of the refractive index separately. To quote: "we would not expect the field in the sphere to be uniform when the external field is a plane wave unless $2\pi\kappa a/\lambda << 1$" where $a = R$, the sphere radius. Note that $2\pi\kappa a/\lambda = \kappa kR$. They then argue that a second condition for Rayleigh scattering is needed because the entire sphere must respond uniformly in time, i.e. sub-volumes in the sphere must oscillate in phase. This condition is based upon the need for the scattered waves from the sub-volumes of the sphere to reach the detector in phase. The result is the requirement that $nkR << 1$. Since the complete refractive index is $m = n + i\kappa$, the combined condition for Rayleigh scattering is $|m|kR << 1$. Now we emphasize that the Rayleigh condition for scattering is that the internal field is homogeneous in amplitude and phase.

In contrast to scattering, absorption is not significantly affected by the real part of the refractive index because absorption is not dependent upon in-phase addition of waves at the detector. Now we emphasize that the Rayleigh condition for absorption is that the internal field is homogeneous in amplitude independent of phase. Thus the Rayleigh condition for absorption is best stated as $\kappa kR << 1$ not $|m|kR << 1$. Rayleigh absorption can occur for all size parameters kR because κ can be very small. Empirically, using the Mie equations, we find $\kappa kR < 0.3$ to be a viable condition for Rayleigh absorption functionality on fundamental physical properties of the sphere.

We have also discovered that Fresnel reflection is relevant for sub-wavelength-size spheres. This is true for the functionality on the physical properties of the sphere and, to a good approximation, for the magnitude. Perhaps this is not so surprising when one considers the fact that both the Mie scattering and Fresnel equations are based on the electromagnetic boundary conditions, the only difference being the different symmetries, spherical and planar, respectively.

Finally, large κ can increase scattering to the detriment of absorption. This is also true for both spheres and planar interfaces.

4. Conclusions

We have studied the absorption cross section for spheres calculated with the Mie equations. We find four regimes of behavior: the Rayleigh Regime, the Geometric Regime, the Reflection Regime, and the Crossover Regime. We have presented simple formulas to describe the absorption in these regimes. Two parameters govern these regimes, the imaginary part of the refractive index, κ, and the ratio of the sphere radius to the optical penetration or skin depth, κkR. For absorption, the Rayleigh regime applies for all particle sizes so long as $\kappa kR < 0.3$. Fresnel reflection occurs whenever both $\kappa > 3$ and $\kappa kR > 3$, and these conditions allow for Fresnel reflection from sub-wavelength-size spheres.

Acknowledgements

The work of CMS was supported by NSF grant AGS-1649783. The work of HM has been supported by NASA EPSCoR under Cooperative Agreement No. NNX14AN24A, NASA ROSES under Grant No. NNX15AI48G, the National Science Foundation under Grant No. AGS-1544425, and the National Science Foundation's Solar Energy-Water-Environment Nexus in Nevada under Cooperative Support Agreement No. EPS- IIA-1301726.

References

[1] Kerker M. The scattering of light, and other electromagnetic radiation. New York: Academic Press; 1969. p. 666. p xv.
[2] Wang G, Chakrabarti A, Sorensen CM. Effect of the imaginary part of the refractive index on light scattering by spheres. J Opt Soc Am A 2015;32:1231–5.
[3] Heinson YW, Maughan JB, Ding JC, Chakrabarti A, Yang P, Sorensen CM. Q-space analysis of light scattering by ice crystals. J Quant Spectrosc Ra 2016;185:86–94.
[4] Sorensen CM, Heinson YW, Heinson WR, Maughan JB, Chakrabarti A. Q-space analysis of the light scattering phase function of particles with any shape. Atmosphere-Basel 2017:8.
[5] Hecht E. Optics. Addison-Wesley: Reading, Mass.; 2002. p. 698. p vi.
[6] Bohren CF, Huffman DR. Absorption and scattering of light by small particles. New York: Wiley; 1983. p. 350. p xiv.
[7] Moosmüller H, Arnott WP. Particle optics in the Rayleigh regime. J Air Waste Manage 2009;59:1028–31.
[8] Moosmüller H, Sorensen CM. Small and large particle limits of single scattering albedo for homogeneous, spherical particles. J Quant Spectrosc Ra 2018;204:250–5.
[9] Moosmüller H, Chakrabarty RK, Arnott WP. Aerosol light absorption and its measurement: a review. J Quant Spectrosc Ra 2009;110:844–78.
[10] Moosmüller H, Arnott WP. Angular truncation errors in integrating nephelometry. Rev. Sci. Instrum. 2003;74:3492–501.
[11] Moosmüller H, Arnott WP. Erratum: "Angular truncation errors in integrating nephelometry. Rev. Sci. Instrum. 2003;74:3492 Rev. Sci. Instrum. **2019**, 90, 019901.
[12] Mishchenko MI, Travis LD, Lacis AA. Scattering, absorption, and emission of light by small particles. Cambridge university press; 2002.
[13] van de Hulst, H.C. Light scattering by small particles. Wiley: New York„ 1957; p 470 p.
[14] Chylek P, Zhan JY. Interference structure of the Mie extinction cross-section. J Opt Soc Am A 1989;6:1846–51.
[15] Lock JA, Yang L. Interference between diffraction and transmission in the Mie extinction efficiency. J Opt Soc Am A 1991;8:1132–4.
[16] Moosmüller H, Sorensen CM. Single scattering albedo of homogeneous, spherical particles in the transition regime. J Quant Spectrosc Ra 2018;219:333–8.